Journal of Manufacturing Processes xxx (xxxx) xxx–xxx

Contents lists available at ScienceDirect

Journal of Manufacturing Processes

journal homepage: www.elsevier.com/locate/manpro

Experimental and numerical investigation on a new FSW based metal to composite joining technique

Dario Baffari*, Gianluca Buffa, Davide Campanella, Ernesto Lo Valvo, Livan Fratini

Department of Industrial and Digital Innovation – University of Palermo, Viale delle Scienze, Ed. 8, 90128, Palermo, Italy

ARTICLE INFO

Keywords:
FSW
Dissimilar joint
Aluminum Alloy
Thermoplastic composite
Polypropylene

ABSTRACT

In the last decades, different techniques were proposed to join aluminum sheets with composites materials. Each of them has advantages and weak points over the others and new techniques and patents are continuously developed to overcome these difficulties. In this paper an experimental and numerical investigation on a new Friction Stir Welding based approach to mechanically join AA6082-T6 to self-reinforced polypropylene is presented. The aluminum sheet is pre-holed along both the sides of the weld line and a pinless tool generates the heat and pressure needed to prompt back-extrusion of the composite. New experimental fixtures and hole designs were investigated in order to enhance the mechanical resistance of the joints and a numerical model was set up to study the process mechanics.

1. Introduction

Effective joint between composite panels and metal alloys is a necessity for the production of lightweight hybrid structures in many industrial fields such as automotive, aeronautics and shipbuilding [1]. To face this issue, conventional techniques to join non-metallic and metallic parts have been widely investigated in the past with particular focus on mechanical fastening and the use of adhesive bonding.

Mechanical fastening using rivets or other external joining elements is commonly used because of its simplicity and easy disassembling. The main weakness of this techniques consists in the through hole which causes stress concentration [2] enhancing crack nucleation, resulting in premature failure. The difficulties in joining dissimilar materials and the limitations of the conventional techniques to join effectively complex geometries prompted many researchers to investigate new joining technologies [3]. Self-piercing riveting (SPR) is one of the innovative methods, proposed in the last decades, which is currently being used in automotive and aerospace industries to obtain hybrid joints between steel and aluminum plates [4]. In SPR, the tubular rivet perforates the top plate driven by a punch and deforms the lower sheet against a specifically designed die. Rivet shank is subjected to severe plastic deformation inside the bottom element as the punch progresses reinforcing the joint itself. The whole process is carried out in a single operation since pre-drilled holes are not required [5,6]. Thus, there is no need for exact alignment between the plates and riveting apparatus. As SPR joints effectiveness is highly dependent on the interlock with the base layer materials, rivets should be inserted from thin to thick sections and from hard to soft panels in order to obtain optimal results. Nevertheless, it should be observed that as far as self-pierce riveting (or riveting) is regarded an increase in weight is given to the assembled part due to the addition of the rivet itself. To face that issue, some researcher [7] proposed to use clinching to join AA5053 to polystyrene but additional problems aroused due to the lower enveloping effect of the polymer during the upsetting phase which enables crack formation. Abibe et al. [8] investigated a modified version of the clinching technology, namely Injection Clinching Joining (ICJ), where a protruding stud on the polymeric plate is formed by a hot die in a sort of rived going through a pre-drilled hole in the metal sheet. Drawbacks of the process are the further operations needed to produce the extruded stud and the spot joining nature of the process.

Regarding the use of adhesive bonding, it is worth pointing out that the chosen adhesives must have good wettability with respect to the materials to be joined, such as carbon fiber reinforced polymer (CFRPs) and aluminum alloys, which are generally in a semi-solid state to facilitate associated applications [9]. However, to fabricate load bearing joints, liquid adhesives have to be used, which have inbuilt ability to harden without curing at elevated temperatures. Seong et al. [10] highlighted the effect of a few process parameters, i.e. bonding pressure, overlap length, adherent thickness, and material type on the mechanical properties of AA2024-T3 and three types of prepegs (SK Chemical USN125 carbon/epoxy, WSN-3k carbon fabric and GEP125 glass fabric). The use of adhesives allows to obtain a continuous contact between the surface of the parts, which results in structures characterized by uniform stress distribution and good mechanical

* Corresponding author.
E-mail address: dario.baffari@unipa.it (D. Baffari).

https://doi.org/10.1016/j.jmapro.2018.03.048
Received 30 November 2017; Received in revised form 23 February 2018; Accepted 15 March 2018

performance under tension, compression and shear [11]. However, the need for extensive surface treatments increases the overall cost of the process and is quite time consuming. For example, in case of aluminum alloys, the formation of superficial layer of aluminum oxide (Al_2O_3) is unavoidable upon exposure to air or water, resulting in very low wetting capability. Such tenacious films are hard to remove without extensive chemical treatment [12]. Therefore, the surface should be chemically modified in order to prevent such oxides formations in the first place. This can be done either by adding coupling reagents or by anodizing the surfaces [13]. Coupling reagents determine strong and irreversible covalent bonds between surface oxides and hydroxides, which link themselves with adhesive during the curing process. Recently, a few different research group started investigating new joining techniques based on the Friction Stir Welding process (FSW) to produce hybrid metal-composite joints. Liu et al. used FSW to produce lap joint between AA6061 aluminum alloy and monomer casting nylon (MC Nylon-6). The bonding occurs thanks to the local melting of the plastic due to the heat generated by the tool and the subsequent cooling under the forging action of the tool itself [14]. In 2014, Goushegir et al. proposed to apply the Friction Spot Joining technique (FSpJ) to join AA2024 and AA6061 aluminum alloys to carbon fiber reinforced poly [15,16]. In the FSpJ process, the tool is made of three different parts: a clamping ring, which holds the sheets to join, a rotating sleeve, which softens the sheet metal (placed on top of the joint) till its bottoms surface, and a rotating and independent pin which is used to press the extruded material and consolidate the weld. Successively, Yusof et al. demonstrate the feasibility of AA5052 to PET joint using the same technology [17]. Although effective, FSpJ process resulted to be quite expensive and complex to be carried out as the tool is composed of three separate parts that need to rotate and plunge independently.

In 2016 [18] the authors of this paper proposed an innovative friction stir welding based technology to produce dissimilar aluminum to thermoplastic self-reinforced composite joints. The aluminum sheet is pre-holed along both the sides of the weld line. A pinless tool generates the heat and pressure needed to activate a back-extrusion mechanics of the composite panel. Joints have been produced with varying holes diameter and pitch. It has been demonstrated that in such kind of process the mechanical fastening is the dominant fastening mechanism assuring the effectiveness of the joint. Actually, no bonding or adhesion is obtained between the resin of which is made the composite panel and surface of the sheet metal blank.

In this study, a further variation of this process is used to join AA6082-T6 aluminum alloy to self-reinforced polypropylene composite panel. Geometrical parameters of the holes were varied and the mechanical properties of the joints were analyzed. Additionally, two plates were placed on top of the upper plate in order to confine the extrusion in the drilled holes. A dedicated numerical model was set up and used to study the process mechanics, highlighting the distribution of the main field variables, such as temperature, strain and strain rate as well as the occurring material flow determining the mechanical fastening.

2. Materials and Methods

2.1. Materials

The used metallic material, i.e. the sheet metal blank, is a 6082-T6 aluminum alloy, 3 mm in thickness. This Si-Mg aluminum alloy is widely used in automotive and transportation industries because of its good mechanical strength and corrosion resistance. Table 1 show the main mechanical and thermal properties of AA6082-T6

The composite material is 100% self-reinforced polypropylene (Curv® produced by PROPEX Fabrics), 2.7 mm in thickness. Fibers were textured with a 90° angle in order to have the same properties in the two orthogonal directions. Table 2 shows the main mechanical and thermal properties of the considered composite material.

Table 1
Mechanical and Thermal properties of the AA6082-T6.

Material Density [g/cm^3]	Tensile Modulus [MPa]	Tensile Strength [MPa]	Tensile Strain to Failure [%]
2.71	69000	310	11
Melting Temperature [$^\circ C$]	Heat Capacity [$N/mm^2\ ^\circ C$]	Thermal Conductiv [$N/sec\ ^\circ C$]	Thermal Expansion [$10^{-5}\ ^\circ C^{-1}$]
650	2.43	180	2.2

Table 2
Mechanical and Thermal properties of the Curv®.

Material Density [g/cm^3]	Tensile Modulus [MPa]	Tensile Strength [MPa]	Tensile Strain to Failure [%]
0.91	3000	140	17
Melting Temperature [$^\circ C$]	Heat Capacity [$N/mm^2\ ^\circ C$]	Thermal Conductiv [$N/sec\ ^\circ C$]	Thermal Expansion [$10^{-5}\ ^\circ C^{-1}$]
180	1.74	0.4	7.0

2.2. Experimental set up

The experimental campaign was carried out on a ESAB LEGIO FSW 3ST, a dedicated 2 axes Friction Stir Welding machine. The contact force condition is controlled by the PLC, which provides a dedicated closed-loop controller for this crucial process parameter.

A pinless tool, 29 mm in diameter, was used. The tool was plunged into the aluminium sheet and moved along the longitudinal direction with constant feed rate. Bonded specimens were made by overlapping plates placing the composite material at the bottom of the joint while the aluminium plate was placed on top. The heat generated by the friction forces work softens the top sheet and is transferred by thermal conduction to the bottom sheet. As the tool advances, backward extrusion occurs in the composite panel, corresponding to the holes in the aluminium sheet, due to the vertical force exerted by the tool itself and the clamping fixture [18].

Two parallel rows of holes were drilled on the aluminium sheet with diameter equal to 5 mm and pitch 10 mm. Fig. 1 shows a sketch of the joint highlighting the position of the weld seam and the holes. The transverse distance between the holes was kept constant and equal to 44 mm.

The investigated process parameters were chosen on the basis of the

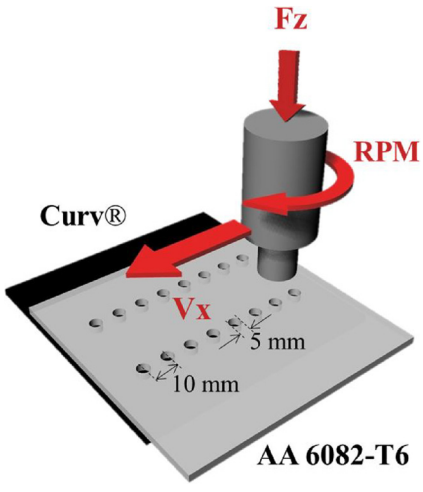

Fig. 1. Sketch of the process.

Table 3
Geometrical and technological parameters used.

Tool rotation [*rpm*]	Feed rate [*mm/min*]	Tilt angle [*deg*]	Tool force [*N*]	Dwell time [*s*]
1000	100	2	3000	1.5
Holes diameter [*mm*]	Holes pitch [*mm*]	AA6082 thickness [*mm*]	Curv ® thickness [*mm*]	Tool plunging speed [m/s]
5	10	3	2.7	0.05

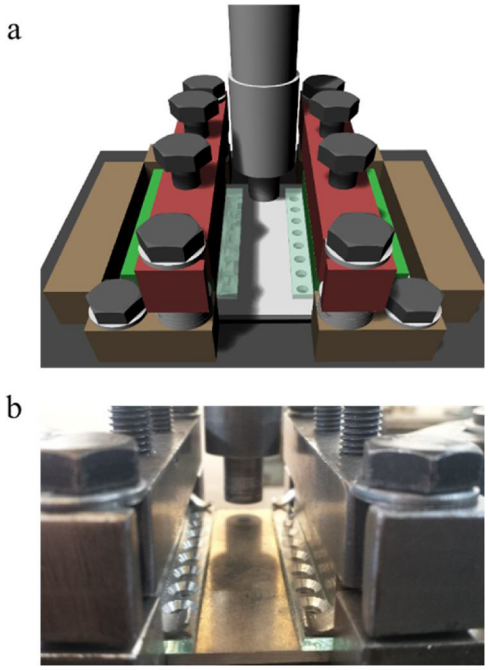

Fig. 2. (a) Design and (b-c) actual build of sheet fixing system.

former experiments carried out on the process and were determined through and optimization procedure aimed to maximized the shear resistance of the joints [18]. Table 3 shows the geometrical and technological parameters used for the experiments.

Fig. 2 shows the especially dedicated clamping system which was designed and built just for the carried out experimental campaign

To ensure the correct distribution of pressure on the sheet metal during the process, a metal block was placed between the plates and the pressure screw that ensured the restraining forces (Fig. 3).

Two plates were placed on top of the upper plate in order to limit the extrusion inside the drilled holes. This allowed to prevent the formation of overhanging extrudates (Fig. 4a) that that may affect the usability of the joint in visible areas or in complex structures or which would require a further finishing operation to be carried out after the joining process.

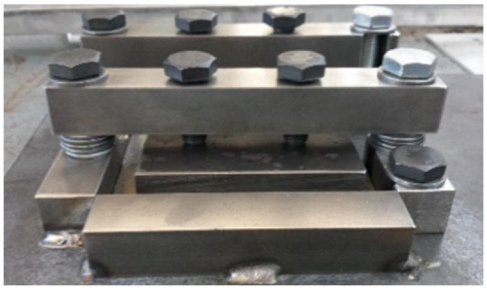

Fig. 3. Pressure screw fixture.

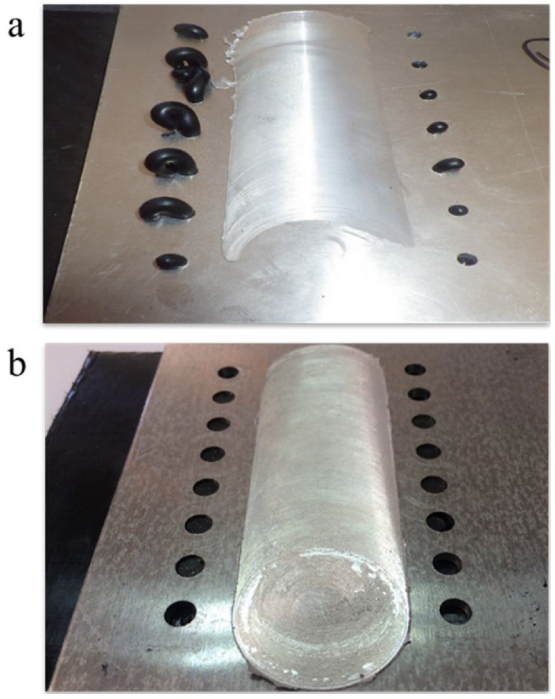

Fig. 4. Joints obtained without (a) and with (b) the backing plate.

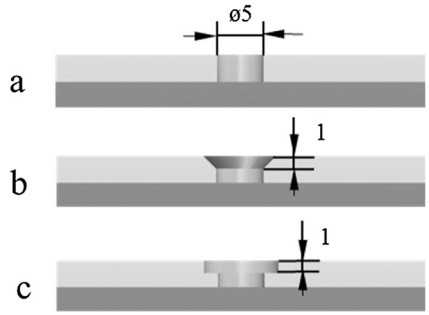

Fig. 5. Holes geometry: (a) cylindrical (b) countersunk (c) counterbore.

Three different holes shape were investigated during the experimental campaign, i.e. cylindrical, counterbore and countersunk (Fig. 5). Additionally, in order to reduce the stress concentrations, a chamfer on the bottom side of the metal sheet was drilled.

3. Numerical model

A previously developed numerical model [18] was updated in order to keep into account the new experimental setup and holes geometry. The thermo-mechanical coupled model was implemented on the commercial FEM software SFTC DEFORM-3D, a lagrangian implicit solver meant to deal with bulk metal forming processes and widely used to simulate solid-bonding based welding technologies (i.e. FSW, FSE, LFW etc.). Contrary to the conventional FSW simulations, the used model is not characterized by a single block approach since the polypropylene flow stress has to be properly taken into account. Both the two materials were characterized using a rigid-visco-plastic model with Von Mises yield criterion. The associated equations are:

$$\dot{\bar{\varepsilon}}_{ij} = \frac{3\dot{\bar{\varepsilon}}\sigma_{ij}^{'}}{2\bar{\sigma}} \tag{1}$$

$$\bar{\sigma} = \sqrt{\frac{3}{2}}\{\sigma_{ij}\sigma_{ij}\}^{\frac{1}{2}} \tag{2}$$

Table 4
Material constants for the temperature, strain and strain rate dependent flow stress.

Material	a	c_1	c_3	c_4	c_5	n
AA6082	−62.3	1367.8	0.0002	1.10E-5	−1130.7	−0.002
Curv®	−3.6	195.1	0.2380	−152413	1454.9	3.032

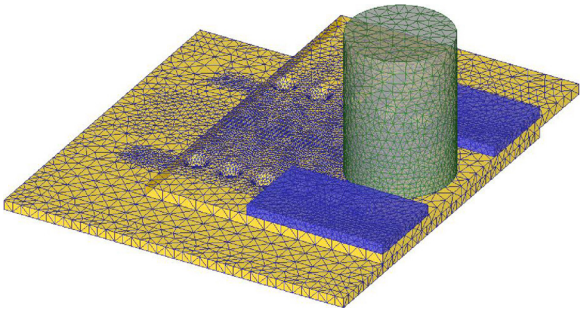

Fig. 6. Assembled model at the beginning of the simulation with partial section to show the meshing of each component.

$$\dot{\bar{\varepsilon}} = \sqrt{\frac{3}{2}}\{\dot{\varepsilon}_{ij}\dot{\varepsilon}_{ij}\}^{\frac{1}{2}} \tag{3}$$

where the effective stress depends on temperature, strain and strain-rate:

$$\bar{\sigma} = a + c_1\exp[-c_3 T + c_4 T\ln(\dot{\bar{\varepsilon}})] + c_5\varepsilon^n \tag{4}$$

The data for the aluminum alloy were extracted form DEFORM library, while a new material model for the polypropylene was created using datasheet given by the producer (Table 4).

In addition to the pinless tool and the sheets to be welded, two backing plates, modelled as rigid objects, were placed on top of the holes in order to act as a barrier to the polypropylene back extrusion flow. In Fig. 6 the meshing of the different objects is showed, highlighting the refinement in the elements size in the area interested by high deformation (i.e. the composite extrusion area). In particular, a minimum mesh size of 1 mm was selected and a total of 10000 tetrahedral elements was used for both the polypropylene sheet and the aluminium one.

4. Results and Discussions

For all the three investigated holes geometries, a complete aluminum holes cavity filling with extruded polypropylene was observed. In order to assess the mechanical resistance of the joints, shear tests were carried out. Spacing tabs were added in order to reduce the effect of undesired bending stress. Five repetitions were carried out for each of the considered case-studies.

Fig. 7 shows the average results of the shear tests with the three considered holes geometries. Although the three case studies show a comparable maximum elongation, a significant difference is observed for the maximum failure force. It is seen that cylindrical holes resulted in lower mechanical resistance with respect to the other case studies. Looking at the joints after the shear tests, it is observed that the cylindrical extruded pins were merely damaged during the shear test (Fig. 8), while counterbored pins were completely cut off at the base layer (Fig. 9). This implies that a “pullout” failure mode [18] occurs for the former, while an “interfacial” failure mode, with the complete shearing of the extruded material, is obtained for the latter. For this condition, the obtained mechanical fastening is stronger than the composite material itself.

The reasons for the shown resistance behavior of the joints can be investigated by analyzing the numerical model results. The numerical

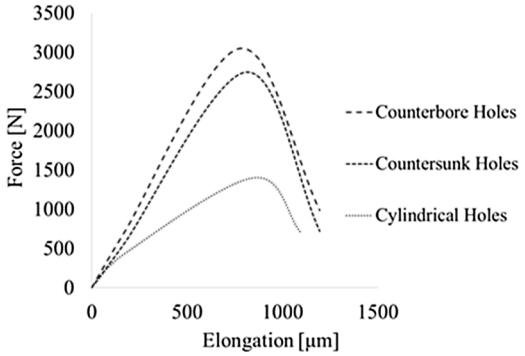

Fig. 7. Shear test results with varying holes geometry.

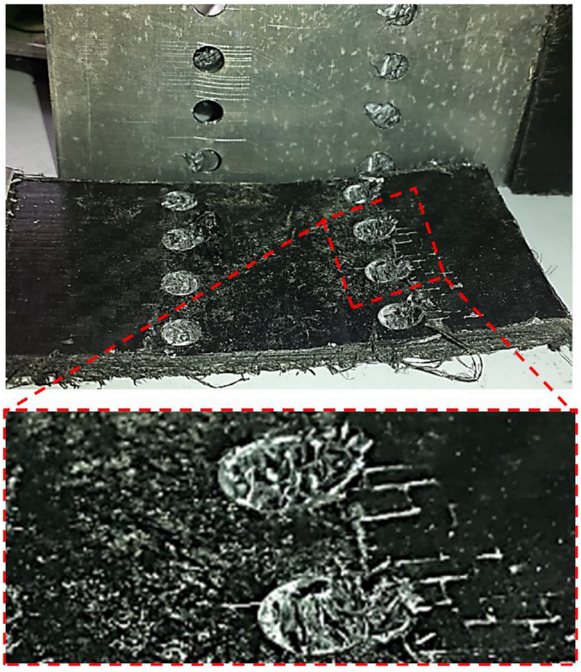

Fig. 8. Shear tests samples for the cylindrical hole geometry.

model was tuned against temperature measurements using a K-type thermocouple embedded into the aluminum plate. In particular, the tribological conditions (i.e. the shear friction factor) and heat exchange coefficients between the different objects constituting the model were varied in order to match the experimental temperature measurements with the FEM result obtained through the point tracking option. Fig. 6a shows the temperature distribution in the composite sheet, while a comparison between the experimental temperature history and the numerically calculated one is reported in Fig. 10b.

The numerical model is capable of predicting the distribution of the most relevant field variable and the evolution of the material flow during the process, with particular emphasis on the proper filling of the holes in the upper plate. Fig. 11 shows the resulting geometry of the polypropylene extrudates at the end of the process with varying the holes geometry.

In particular, looking at the strain distribution in the three case studies (Fig. 12), it is clear that the countersunk and the counterbore (Fig. 12b and c, respectively) geometries cause the polypropylene to undergo larger deformation during the backward extrusion process.

The different level of deformation can be attributable to the holes geometries. Fig. 13 highlights how the concave geometry of the counterbore and the presence of the backing plate deviate the material flow creating a sort of “rivet” of polypropylene, characterized by material continuity with the bottom sheet and resulting in increased overall

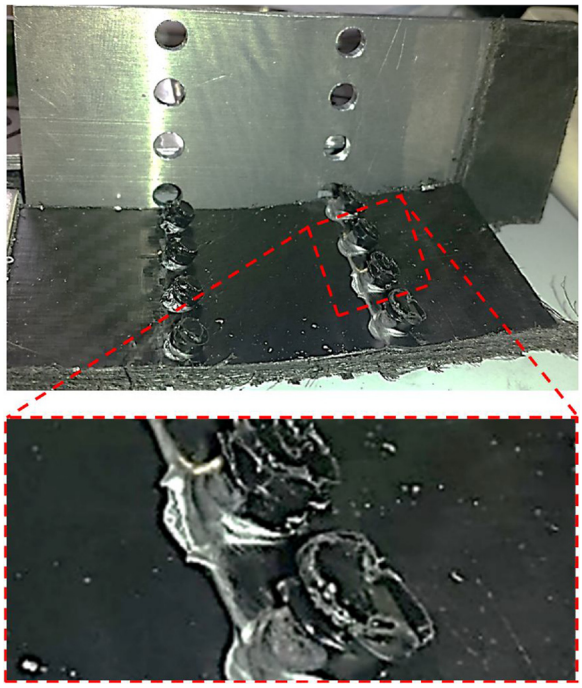

Fig. 9. Shear tests samples for counterbore.

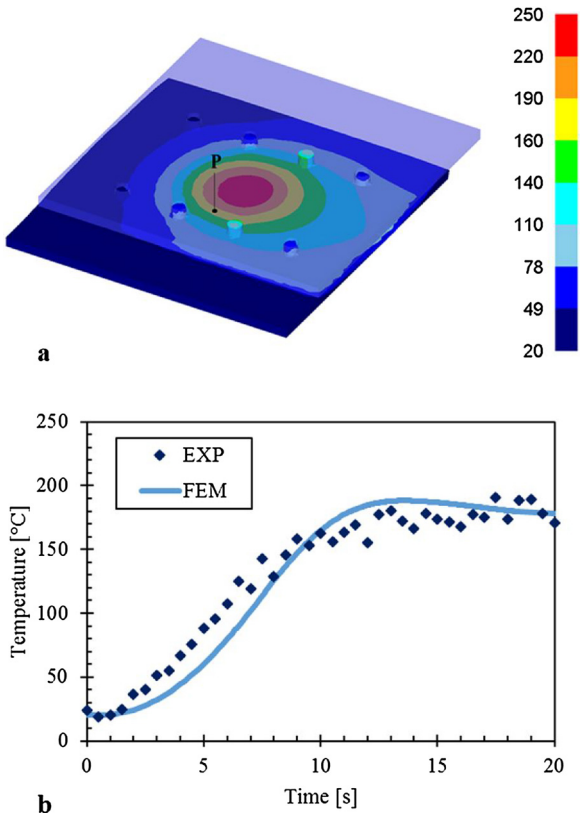

Fig. 10. (a) Typical temperature distribution with measurement point (P) and (b) FEM and experimental results comparison.

strain with respect to the simpler cylindrical hole. Hence, the counterbore geometry, as already highlighted by the shear test, also significantly increases the joint resistance by creating a physical obstacle to the pull out of the extrudates a more effective mechanical fastening is obtained with such geometry.

It is worth noticing that the strain distribution on the transversal

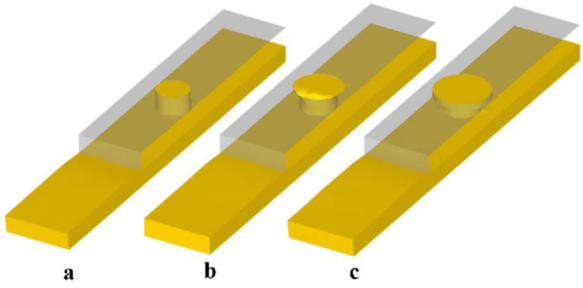

Fig. 11. Geometry of the joint at the end of the simulation (partial transversal view) for the (a) cylindrical, (b) countersunk, and (c) counterbore case studies.

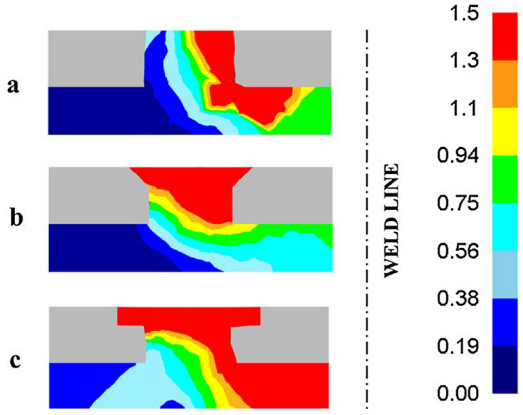

Fig. 12. Von Mises strain distributions (partial transversal section) for the (a) cylindrical, (b) countersunk, and (c) counterbore case studies.

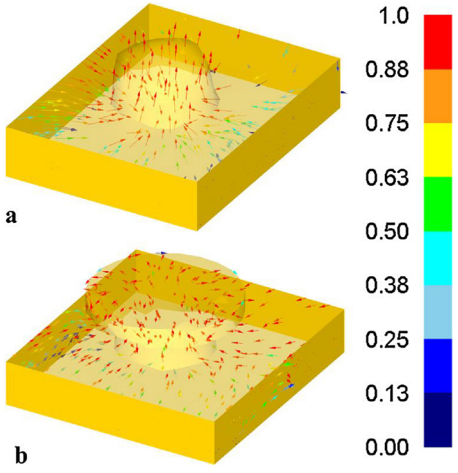

Fig. 13. Material flow during the process (partial view) for the (a) cylindrical and (b) counterbore case studies.

section of the extrudates (Fig. 12) presents a clear asymmetry. This can be explained analyzing the velocity filed near the extrudates area (Fig. 14b); material coming from the weld line side is characterized by a higher velocity and undergoes higher deformation with respect to the material coming from the external side of the composite sheet. This asymmetric behavior is imputable to the temperature distribution (Fig. 14a) in the composite sheet. The polypropylene closer to the tool is heated and softened more than the one in the peripheral area, resulting in a more conspicuous flow that fill the holes cavity from the unevenly while the extrusion takes place (Fig. 15).

The shear tests carried out on the obtained joints were simulated in order to highlight the different failure modes. In Fig. 16a it is shown how the cylindrical extrudates tend to slip off of the hole causing the

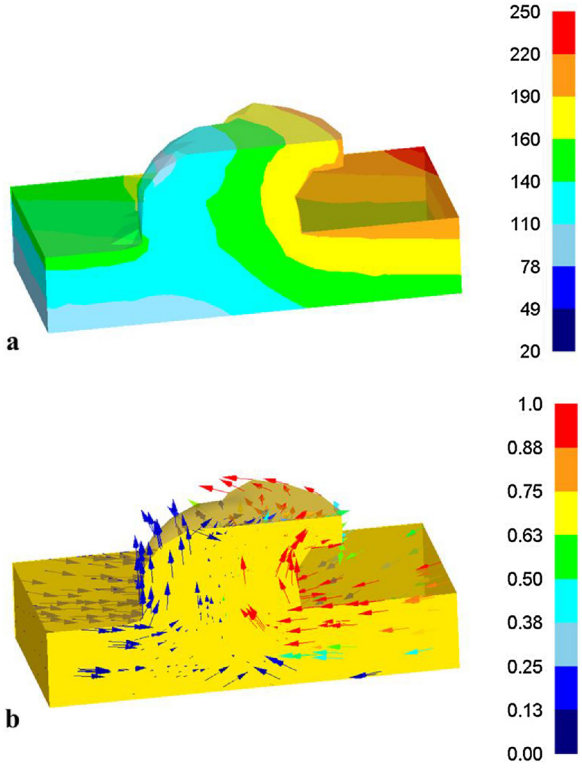

Fig. 14. (a) Material flow during the process (partial view) and (b) corresponding temperature distribution for the counterbore case study.

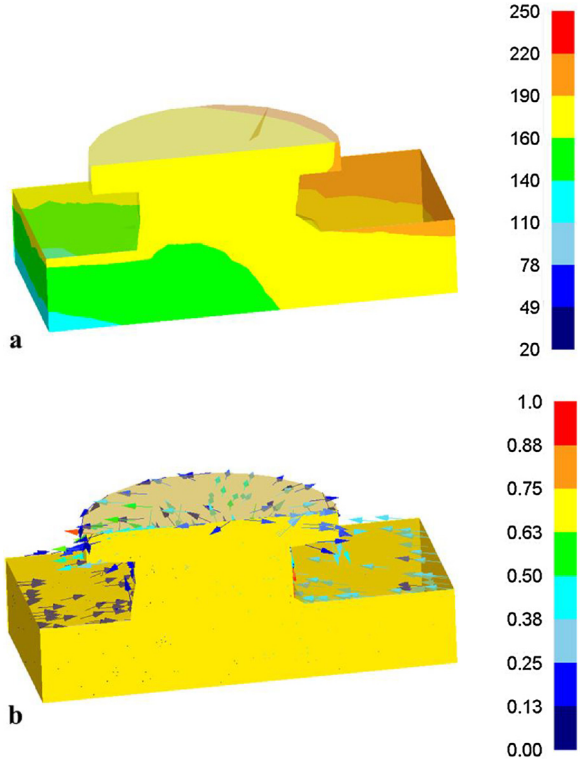

Fig. 15. (a) Material flow at the end of the process (partial view) and (b) corresponding temperature distribution for the counterbore case study.

significant increase of the effective tensile field in the joint area since a secondary bending effect is added to the shear stress. This effect is not observed in the countersunk and the counterbore case studies (Fig. 16b and c, respectively) that allowed to obtain the higher resistance since

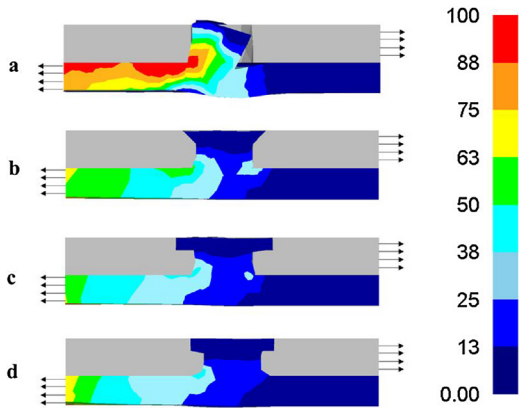

Fig. 16. Simulated shear test (partial transversal section) for the (a) cylindrical, (b) countersunk, (c) counterbore, and (d) counterbore with chamfer case studies after 10 mm of elongation.

the "head" on top of the extrudates prevented the pulling out and the bending of the polypropylene stud. It is worth noticing how the introduction of a small chamfer on the opposite side of the plate with respect to the bore allows to further reduce the effective stress and the stress concentration at the base of the polypropylene extrudates (Fig. 16d). For the latter condition, a further increase in the joint resistance was observed, with maximum failure load equal to 3260 N.

5. Conclusion

In the paper, the results of an experimental and numerical campaign aimed at the enhancement of the mechanical properties of dissimilar aluminum /polypropylene composite joints are presented. An innovative Friction Stir welding based process was utilized to produce the joints. A dedicated numerical model, able to take into account the presence of the two different materials, was firstly validated and then used to determine the effect of the process parameters on the material flow and on the distribution of the main field variables. In this way, it was possible to highlight the hole cavity filling in the aluminum sheets during the joining process, forming a sort of polypropylene rivet characterized by material continuity with the bottom sheet of the joints. The produced joints, in according with the flow predicted by the numerical model, showed a complete filling of the cavities. What is more, for the countersunk and counterbore configurations, a significantly enhanced joint strength was obtained with respect to the cylindrical case study. Finally, the introduction of a chamfer at the base of the hole drilled in the aluminum sheets, allowed for further enhancement of the joint mechanical properties due to a reduction of the stress concentration in this area during the shear tests.

The proposed solution can be considered feasible for an industrial point of view and further CAE of the joints can be carried out. During the process, local thinning of the composite panel may occur and should be also taken into account depending on the specific geometrical issues of the hybrid part to be produced. Furthermore, as a future development, the feasibility of the process for joining different kind of thermoplastic composites (i.e. not just self-reinforced) has to be investigated. This could expand the potential of this joining technology to structural primary junction.

References

[1] Alberti EA, Da Silva LJ, D'Oliveira ASCM. Soldag E Insp 2014;19:190–8.
[2] Amancio-Filho ST, Dos Santos JF. Polym Eng Sci 2009;49:1461–76.
[3] Messler RW. Mater Des 1995;16:261–9.
[4] Pramanik A, Basak AK, Dong Y, Sarker PK, Uddin MS, Littlefair G, Dixit AR, Chattopadhyaya S. Compos Part A Appl Sci Manuf 2017;101:1–29.
[5] Hoang NH, Porcaro R, Langseth M, Hanssen AG. Int J Solids Struct 2010;47:427–39.
[6] Di Franco G, Fratini L, Pasta A. Int J Adhes Adhes 2013;41:24–32.

[7] Lambiase F. Mater Des 2015;87:606–18.
[8] Abibe AB, Amancio-Filho ST, dos Santos JF, Hage E. Mater Des 2013;46:338–47.
[9] Brockmann W, Hennemann OD, Kollek H, Matz C. Int J Adhes Adhes 1986;6:115–28.
[10] Seong MS, Kim TH, Nguyen KH, Kweon JH, Choi JH. Compos Struct 2008;86:135–45.
[11] Adderley CS. Mater Des 1988;9:287–93.
[12] Pramanik A, Basak AK. Stainless Steel: Microstructure, Mechanical Properties and Methods of Application. 2015.
[13] Kim G, Ajersch F. J Mater Sci 1994;29:676–81.
[14] Liu FC, Liao J, Nakata K. Mater Des 2014;54:236–44.
[15] Goushegir SM, dos Santos JF, Amancio-Filho ST. Mater Des 2014;54:196–206.
[16] Goushegir SM. Weld World 2016;60:1073–93.
[17] Yusof F, Miyashita Y, Seo N, Mutoh Y, Moshwan R. Sci Technol Weld Join 2012;17:544–9.
[18] Buffa G, Baffari D, Campanella D, Fratini L. Procedia Manuf 2016;5:319–31.